JOURNAL OF GEOPHYSICAL RESEARCH, VOL. 112, A07220, doi:10.1029/2007JA012300, 2007

Effect of oblique electromagnetic ion cyclotron waves on relativistic electron scattering: Combined Release and Radiation Effects Satellite (CRRES)-based calculation

G. V. Khazanov[1] and K. V. Gamayunov[1*]

Received 24 January 2007; revised 7 May 2007; accepted 4 June 2007; published 31 July 2007.

[1] We consider the effect of oblique electromagnetic ion cyclotron (EMIC) waves on relativistic electron scattering in the outer radiation belt (RB) using simultaneous observations of plasma and wave parameters from Combined Release and Radiation Effects Satellite (CRRES). The main findings can be summarized as follows. First, in comparison with field-aligned waves, intermediate and highly oblique distributions decrease the range of pitch angles subject to diffusion and reduce the local scattering rate by about an order of magnitude at pitch angles where the principle $|n| = 1$ resonances operate. Oblique waves allow the $|n| > 1$ resonances to operate, extending the range of local pitch angle diffusion down to the loss cone, and increasing the diffusion at lower pitch angles by orders of magnitude. Second, the local diffusion coefficients derived from CRRES data are qualitatively similar to the local results obtained for prescribed plasma/wave parameters. Consequently, it is likely that the bounce-averaged diffusion coefficients, if estimated from concurrent data, will exhibit the dependencies similar to those we found for model calculations. Third, in comparison with field-aligned waves, intermediate and highly oblique waves decrease the bounce-averaged scattering rate near the edge of the equatorial loss cone by orders of magnitude if the electron energy does not exceed a threshold ($\sim$2–5 MeV) depending on specified plasma and/or wave parameters. Lastly, for greater electron energies, oblique waves operating the $|n| > 1$ resonances are more effective and provide the same bounce-averaged diffusion rate near the loss cone as field-aligned waves do.

Citation: Khazanov, G. V. and K. V. Gamayunov (2007), Effect of oblique electromagnetic ion cyclotron waves on relativistic electron scattering: Combined Release and Radiation Effects Satellite (CRRES)-based calculation, *J. Geophys. Res.*, *112*, A07220, doi:10.1029/2007JA012300.

1. Introduction

[2] The flux of outer zone relativistic electrons (above 1 MeV) is extremely variable during geomagnetic storms. The competition between source and loss, both of which are enhanced during storm periods, determines the resulting relativistic electron flux level in the Earth's outer radiation belt (RB) [e.g., *Reeves et al.*, 2003; *Summers et al.*, 2004; *Green et al.*, 2004]. Usually, the flux falls by up to two or three orders of magnitude during main phase, and gradually increases over a period of a few days during storm recovery phase [e.g., *Meredith et al.*, 2002]. Analyzing 256 geomagnetic storms during the period of 1989–2000, *Reeves et al.* [2003] found that 53% of storms lead to higher flux during the storm recovery phase in comparison to prestorm levels, 28% produce no change, and 19% lead to a net decrease in flux. The large electron flux decrease during the main storm phase is usually associated with a decrease of disturbance storm-time (Dst) index when the relativistic electrons adiabatically respond to the stretching of the magnetic field lines caused by the formation of a partial ring current (RC) [*Kim and Chan*, 1997], and/or a drift out the magnetopause boundary [*Li et al.*, 1997], and/or nonadiabatic scattering into the loss cone due to cyclotron interaction with electromagnetic ion cyclotron (EMIC) waves [*Thorne and Kennel*, 1971; *Lyons and Thorne*, 1972; *Summers and Thorne*, 2003; *Albert*, 2003; *Thorne et al.*, 2005] and/or whistler-mode chorus/hiss waves [e.g., *Summers et al.*, 2007].

[3] Precipitation of outer RB electrons due to resonant pitch angle scattering by EMIC waves is considered to be one of the most important loss mechanisms. Recently, data from balloon-borne X-ray instruments provided indirect but strong evidence for the ability of EMIC waves to cause precipitation of outer zone relativistic electrons in the late afternoon-dusk magnetic local time (MLT) sector [*Foat et al.*, 1998; *Lorentzen et al.*, 2000; *Millan et al.*, 2002]. These observations stimulated theoretical and statistical studies which demonstrated that this mechanism of

[1]National Space Science and Technology Center, National Aeronautics and Space Administration Marshall Space Flight Center, Space Science Department, Huntsville, Alabama, USA.

0148-0227/07/2007JA012300$09.00

*The order of the authors is correct here and throughout. The article as originally published is online.

MeV electron pitch angle diffusion can operate in the limit of strong diffusion and can compete with adiabatic depletion caused by the Dst effect during the initial and main phases of the storm [*Summers and Thorne*, 2003; *Albert*, 2003; *Meredith et al.*, 2003; *Loto'aniu et al.*, 2006].

[4] Although the effectiveness of relativistic electron scattering depends strongly on EMIC wave spectral properties, unrealistic assumptions regarding the wave angular spread were made in previous theoretical studies. Namely, only strictly field-aligned or quasi-field-aligned waves were considered as a driver for electron precipitation [e.g., *Summers and Thorne*, 2003; *Albert*, 2003; *Loto'aniu et al.*, 2006]. The effect of oblique EMIC waves on relativistic electron scattering was recently discussed by *Glauert and Horne* [2005]. For prescribed plasma and wave parameters, considering the H^+-mode EMIC waves, they calculated the equatorial diffusion coefficients and demonstrated that when a realistic angular spread of propagating waves is taken into account, electron diffusion at ~0.5 MeV is only slightly reduced compared to the assumption of field-aligned propagation, but at ~5 MeV, electron diffusion at pitch angles near 90° is reduced by a factor of 5 and increased by several orders of magnitude at pitch angles 30°–80°. As a result, EMIC waves should flatten the pitch angle distribution.

[5] Thus, at energies of a few megaelectronvolts, the assumption of field-aligned propagation breaks down, significantly overestimating the pitch angle diffusion coefficient at large pitch angles, while underestimating the local diffusion rate at smaller pitch angles by orders of magnitude. This is a very strong effect, so in contrast to the paper of *Glauert and Horne* [2005], it is important to consider the impact of oblique EMIC waves on relativistic electron scattering using simultaneous observations for plasma/wave parameters, and to estimate the effect of bounce averaging. In the present study, we calculate the pitch angle diffusion coefficients using plasma and wave parameters observed by CRRES and reported by *Loto'aniu et al.* [2006].

[6] This article is organized as follows. In section 2, we verify the pitch angle diffusion coefficient calculations comparing our results with published results for both the equatorial and bounce-averaged scattering rates. Then, using model wave spectra for He^+-mode EMIC waves with defined plasma parameters, we consider the effect of the wave-normal angle distribution on relativistic electron scattering. In section 3, using plasma/wave parameters observed by CRRES [*Loto'aniu et al.*, 2006], we present the results of our calculations and analysis of the local pitch angle diffusion coefficients for two selected wave packets. Finally, in section 4, we summarize the main findings of our study.

2. Equatorial and Bounce-Averaged Pitch Angle Diffusion Coefficients: Model Calculations

[7] An extensive statistical analysis of the EMIC events presented by *Meredith et al.* [2003] showed that most of the cases when the minimum resonant electron energy fell below 2 MeV were associated with wave frequencies just below the He^+ gyrofrequency. So we take into account only the He^+-mode EMIC waves in the present study. The model wave frequency spectrum is assumed to be Gaussian,

$$B^2(\omega) \sim \exp\left\{-\frac{(\omega-\omega_m)^2}{\delta\omega^2}\right\}, \quad \omega_{LC} \le \omega \le \omega_{UC} \tag{1}$$

where, following *Summers and Thorne* [2003] and/or *Albert* [2003], $\omega_{LC} = \omega_m - \delta\omega$, $\omega_{UC} = \omega_m + \delta\omega$, $\omega_m = 3\Omega_{O+}$, $\delta\omega = 0.5\Omega_{O+}$, and Ω_{O+} is the gyrofrequency of O^+. In our calculations, the wave-normal angle distribution, $g(\theta)$, is assumed to be a constant inside a specified region and zero otherwise. Below, we consider the following three cases,

$$\begin{aligned} \text{Case A (field-aligned):} &\quad 0^\circ \le \theta < 30^\circ,\ 150^\circ < \theta \le 180^\circ, \\ \text{Case B (intermediate):} &\quad 30^\circ \le \theta < 60^\circ,\ 120^\circ < \theta \le 150^\circ, \\ \text{Case C (oblique):} &\quad 60^\circ \le \theta \le 89^\circ,\ 91^\circ \le \theta \le 120^\circ, \end{aligned} \tag{2}$$

where θ is the wave-normal angle. Note that the diffusion coefficient is a linear function of the wave spectral density, and the sum of Cases A, B, and C describe a situation when EMIC wave energy is evenly distributed over the entire wave-normal angle region $0^\circ \le \theta \le 180^\circ$ (we excluded the region near 90° because of Landau damping by thermal electrons [e.g., *Thorne and Horne*, 1992; *Khazanov et al.*, 2007]). For benchmark purposes, we calculate also the diffusion coefficients for a Gaussian distribution over $x = \tan\theta (0^\circ \le \theta \le 15^\circ)$ which has been used by *Albert* [2003]. In each case, the wave amplitude is normalized to ensure that

$$\int_{\omega_{LC}}^{\omega_{UC}} d\omega \int_0^\pi d\theta B^2(\omega) g(\theta) = 1 \text{ nT}^2. \tag{3}$$

Finally, to specify the ion content, we follow *Summers and Thorne* [2003], *Albert* [2003], *Meredith et al.* [2003], and *Loto'aniu et al.* [2006], and prescribe the ion composition to be 70% H^+, 20% He^+, and 10% O^+ (following [*Meredith et al.*, 2003] we call it a "storm-time" ion composition).

[8] The results obtained using the relativistic version of the diffusion coefficient code of *Khazanov et al.* [2003] are shown in Figure 1. The first row shows the equatorial pitch angle diffusion coefficients and the second row shows the corresponding resonance numbers averaged with the following weights:

$$\left\langle n(E,\alpha) \right\rangle = \frac{\sum_n n\left(\int_{\omega_{LC}}^{\omega_{UC}} d\omega \int_0^\pi d\theta D^n_{\alpha\alpha}(\omega,\theta,E,\alpha)\right)}{\sum_n \left(\int_{\omega_{LC}}^{\omega_{UC}} d\omega \int_0^\pi d\theta D^n_{\alpha\alpha}(\omega,\theta,E,\alpha)\right)}, \tag{4}$$

where E and α are the electron kinetic energy and local pitch angle and $D^n_{\alpha\alpha}(\omega,\theta,E,\alpha)$ is the partial equatorial pitch angle diffusion coefficient, and the third row shows the bounce-averaged diffusion coefficients. Note that resonances $\pm n$ come together because the ω term can be omitted in the quasi-linear resonance condition, $\omega - k_\parallel v_\parallel - n\Omega_e/\gamma = 0$ [e.g., *Summers and Thorne*, 2003], and because the wave spectra are symmetric over $\theta = 90^\circ$. The "Gauss" lines in Figure 1 show the results for a Gaussian distribution over x and reproduce well the equatorial and

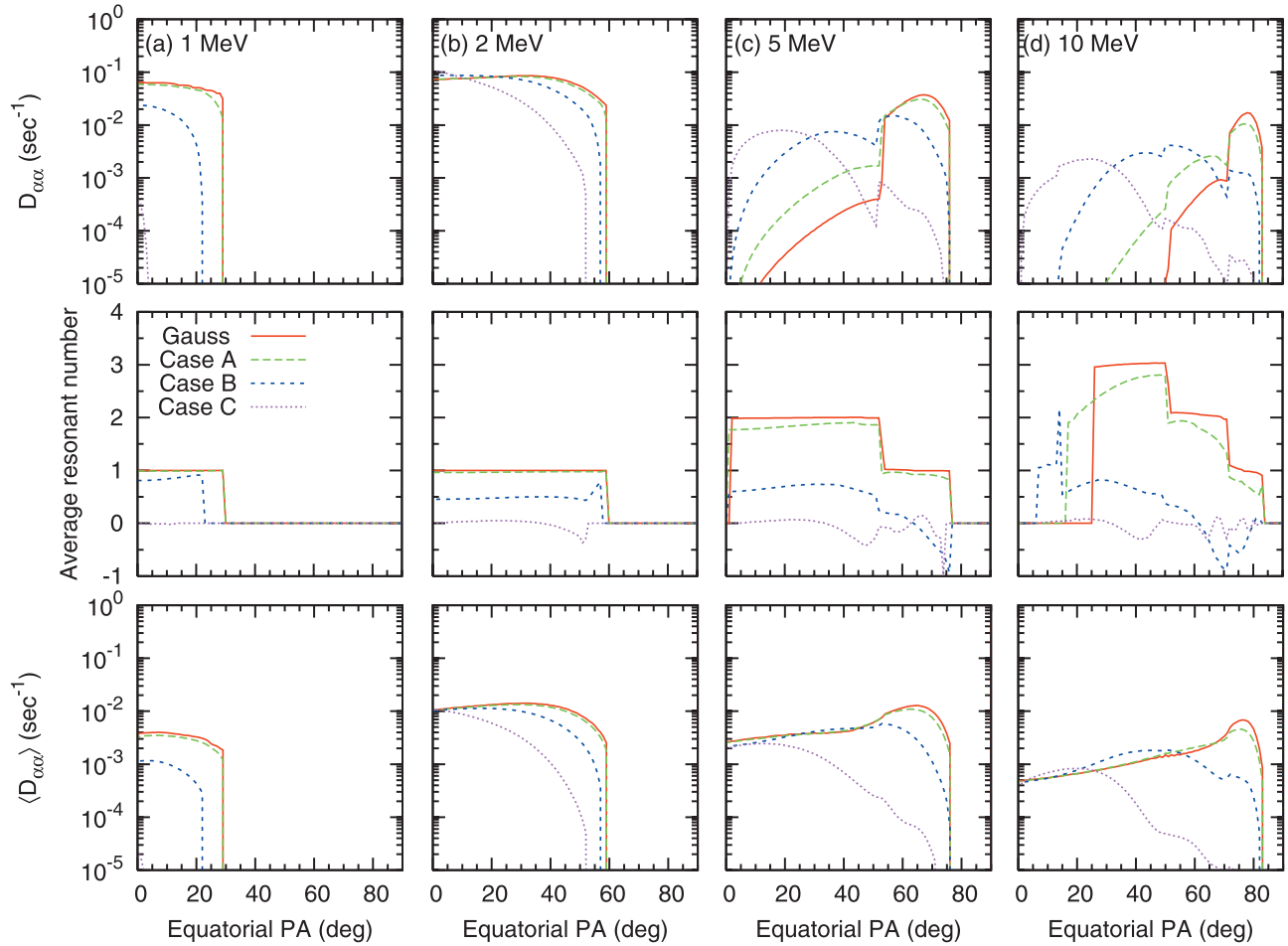

Figure 1. Equatorial and bounce-averaged diffusion coefficients versus equatorial pitch angle for scattering relativistic electrons by the He^+-mode of EMIC waves. Spectral parameters and ion content are given in the text. $L = 4$, and $(\omega_{pe}/\Omega_e)^2 = 10^3$, where ω_{pe} and Ω_e are the equatorial electron plasma frequency and gyrofrequency (without Lorentz factor), respectively. The curve "Gauss" is for a wave-normal angle distribution adopted by *Albert* [2003]. The second row shows the average resonant number weighted by the partial equatorial diffusion coefficient (see the text for definition).

bounce-averaged diffusion coefficients by *Albert* [2003, Figure 6].

[9] Let us first analyze the equatorial pitch angle diffusion coefficients. For all energies, Case A is only slightly less than "Gauss" if only $|n| = 1$ resonances operate, but in the region of $|n| > 1$, it is about five times greater (Figures 1c and 1d, the first row). These dependencies are in good agreement with the previous results by *Albert* [2003, Figure 10, the second row]. For both "Gauss" and Case A, as follows from the second row in Figure 1, the contributions from $n < 0$ are negligible compared with $n > 0$, especially for lower electron energies (see Figures 1a and 1b, the second row). Cases B and C further increase the EMIC wave-normal angle, and as a result, suppress the $|n| = 1$ resonances, and for low energies, they substantially shrink the region of pitch angles subject to diffusion (see Figures 1a and 1b, the first row). At the same time, they increase by orders of magnitude the contribution from $|n| > 1$, which operate for greater electron energies, and cover a greater pitch angle region (see Figures 1c and 1d, the first row). The growing contribution of the $n < 0$ resonances is more pronounced in Cases B and C (in comparison with Case A) because EMIC waves become more elliptically polarized with increasing wave-normal angle (see Figure 1, the second row).

[10] Overall, in comparison with the field-aligned waves, the intermediate and highly oblique wave distributions decrease the pitch angle range subjected to diffusion and reduce the equatorial scattering rate by orders of magnitude for low-energy electrons ($E < 2$ MeV) when only principle $|n| = 1$ resonances operate. For greater electron energies, the $|n| = 1$ resonances operate only in a narrow region at large pitch angles, and despite their greater contribution from field-aligned waves, they cannot support the local electron diffusion into the loss cone. In this case, oblique waves operate on the $|n| > 1$ resonances more effectively and extend the range of pitch angle diffusion down to the loss cone. Note that despite our inclusion of the He^+-mode, the above results are in qualitative agreement with the results of *Glauert and Horne* [2005, Figures 6 and 7] obtained for the equatorial pitch angle scattering by the H^+-mode EMIC waves.

[11] Now we consider the effect of bounce averaging on pitch angle diffusion coefficients. To calculate the bounce-averaged diffusion coefficients, we utilize all the plasma/wave parameters used in the above calculation of the equatorial coefficients, and in addition, a dipole magnetic field model, and the meridional density distribution from *Khazanov et al.* [2006]. We further assume that the EMIC waves are confined to mirror points, and the wave spectra are equatorial.

[12] In all considered cases (see equation (2)), the bounce averaging does not change the shape of the diffusion coefficients for energies below 2 MeV (compare the first and third rows in Figure 1) but simply reduces the pitch angle diffusion rates by an order of magnitude. For energies 5 and 10 MeV, the peak values of the bounce-averaged diffusion coefficients are lower by about a factor of 3 than in the first row of Figure 1. However, the bounce-averaged results for $E > 2$ MeV differ qualitatively from the local coefficients for all wave-normal distributions. Due to significant scattering at higher latitudes, the bounce-averaged diffusion coefficients extend further into the loss cone compared to equatorial results. The bounce-averaged results in Figure 1 demonstrate clearly the effect of EMIC wave-normal angle distribution on relativistic electron scattering.

[13] Recently, *Shprits et al.* [2006] showed that the electron lifetime is most sensitive to the value of the bounce-averaged scattering rate near the edge of the equatorial loss cone, whose value is used to estimate the electron loss timescale [e.g., *Summers et al.*, 2007]. Considering the third row in Figures 1a and 1b, we can see that the intermediate and highly oblique wave distributions reduce the scattering rate near the loss cone by orders of magnitude because only principal $|n| = 1$ resonances operate. For higher electron energies (Figures 1c and 1d) when $|n| > 1$ resonances start to operate, the pitch angle scattering near the edge of the equatorial loss cone depends only slightly on the wave-normal angle distribution, resulting in nearly the same bounce-averaged diffusion rate for all cases. In other words, there is an electron energy, depending on specified plasma and/or wave parameters, which separates lower and higher energy regions with different EMIC wave scattering properties. In the lower energy region, using a field-aligned wave-normal angle distribution leads to a significant overestimate of the diffusion rate compared to oblique waves. In the higher energy region, the scattering rate near the edge of the loss cone almost does not depend on the wave-normal angle distribution.

3. Local Pitch Angle Diffusion Coefficient: CRRES-Based Calculations

3.1. Minimum Resonant Energy

[14] Recently, *Meredith et al.* [2003] presented an extensive statistical analysis of over 800 EMIC events observed on CRRES to establish whether electron scattering can occur at geophysically interesting energies ($\leq$2 MeV). In the absence of specific information on the wave-normal angle, the dispersion relation for strictly field-aligned propagating EMIC waves was used to obtain the electron resonant energy. For consistency, *Meredith et al.* [2003] included only waves with a high ellipticity ($|\epsilon| \geq 0.3$) in the survey. This yielded a subset of 416 events, the majority of which were identified as L-mode. Considering only the central wave frequency, ω_m, in each wave packet, *Meredith et al.* [2003] found that in about 11% of the observations, the electron minimum resonant energy fell below 2 MeV. These cases were restricted to regions where $\omega_{pe}/\Omega_e > 10$ and were associated with wave frequencies just below the helium or proton gyrofrequencies. More recently, trying to increase the above percentage, *Loto'aniu et al.* [2006] considered the entire frequency range for each of the 25 EMIC wave packets observed on CRRES during the initial phase of a geomagnetic storm on 11 August 1991. These authors also used the dispersion relation for strictly parallel propagating EMIC waves and found that, in comparison with results utilizing ω_m only, there are three to four times more wave packets that are able to interact with electrons below 2 MeV.

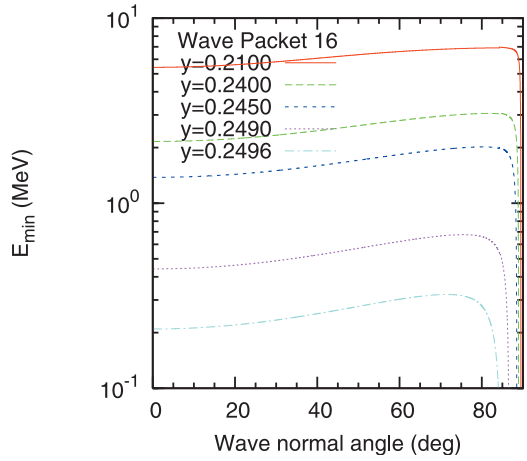

Figure 2. Minimum resonant energy versus normal angle of the He^+-mode EMIC waves. The plasma density and magnetic field are 17 cm^{-3} and 171 nT, taken from the work of *Loto'aniu et al.* [2006, wave packet # 16]. The ion composition is 70% H^+, 20% He^+, and 10% O^+, and the normalized wave frequency is defined as $y = \omega/\Omega_{H^+}$.

[15] The minimum resonant energy depends on the wave-normal angle, and the dependency is stronger in the vicinity of the resonant frequencies where the wave number grows especially fast. Omitting the ω term in a quasi-linear resonance condition ($\omega - k_{||}v_{||} - n\,\Omega_e/\gamma = 0$) and taking $n = 1$, we can obtain the minimum kinetic energy required by electrons for cyclotron resonance interaction with EMIC waves,

$$\frac{E_{min}}{m_e c^2} = \frac{1}{\sqrt{1-\left(\frac{v}{c}\right)^2}} - 1, \quad \left(\frac{v}{c}\right)^2 = \frac{1}{1+\cos^2\theta\left(\frac{kc}{\Omega_e}\right)^2}, \qquad (5)$$

where E_{min} is the minimum kinetic energy, m_e is the electron rest mass, c is the speed of light, and k and v are the wave number and electron velocity. Note that equation (5) can be obtained from equation (7) of *Summers and Thorne* [2003] by omitting the two smallest terms in their equation. To calculate the electron minimum energy, we select the plasma parameters reported by *Loto'aniu et al.* [2006, wave packet # 16], and the results of our calculation are presented in Figure 2. For $\theta = 0°$, as reported in many previous studies

Table 1. Wave Packet and Local Environment Properties Selected From the Work of [*Loto'aniu et al.*, 2006]

Wave packet	$y_m = \omega_m/\Omega_{H+}$	$\delta y = \delta\omega/\Omega_{H+}$	$y_{LC} = y_m - \delta y$	$y_{UC} = y_m + \delta y$	δB^2, nT^2	B_0, nT	N_e, cm^{-3}
16	0.23	0.01	0.22	0.24	2.21	170.9	17
19	0.22	0.02	0.20	0.24	0.84	160.2	15

[e.g., *Summers and Thorne*, 2003], in order to get lower E_{min}, the required wave frequency has to be closer to the He^+ gyrofrequency (in other words, the wave number should be greater). For most wave-normal angles, increasing the angle slightly also increases the minimum energy but there is a dramatic decrease of E_{min} in the region near $\theta = 90°$. This transition boundary depends on the wave frequency. Indeed, there is a resonant wave-normal angle (the angle at which the wave number becomes infinite in the "cold plasma" approximation) for any frequency in the range between Ω_{He+} and the corresponding bi-ion frequency, and this angle is closer to $\theta = 0°$ if the wave frequency is closer to Ω_{He+}. Because of the wave number increase, the resonant energy decreases dramatically in the vicinity of the resonant wave-normal angle, an effect clearly observed in Figure 2. So in cold plasma, E_{min} is lower for oblique or highly oblique wave propagation, depending on wave frequency, than for strictly field-aligned propagating EMIC waves. But, of course, the diffusion coefficient for those wave-normal angles should be significant in order to determine the "physically meaningful" E_{min}, and moreover the cyclotron damping in the vicinity of the He^+ gyrofrequency can be very strong (see below).

3.2. Pitch Angle Diffusion Coefficient

[16] It was demonstrated in section 2 that oblique wave propagation can strongly change the effectiveness of both the local and bounce-averaged relativistic electron scatterings. At the same time, those results were obtained for plasma parameters and wave spectra, which were specified independently. So it is important to consider the effect of using concurrent observational data. In contrast to section 2, we now calculate the local pitch angle diffusion coefficients using the data for plasma and wave parameters reported by *Loto'aniu et al.* [2006].

[17] A long-duration wave event was observed by CRRES on 11 August 1991 in the interval ~0500–0700 universal time (UT) (14.4–15.8 MLT) over a magnetic latitude range of −26° to −24° and L = 6.3–7.6. CRRES was close to apogee in the plasmatrough, and the electron density varied slowly from 12 to 17 cm^{-3}. A total of 25 EMIC wave packets were identified both below and above the local He^+ gyrofrequency [*Loto'aniu et al.*, 2006]. In order to estimate the spectral properties of the wave packets, these authors fitted a Gaussian distribution to the static wave packet transverse power spectral density. Typical FFT data windows and frequency resolutions for the static spectrograms were 100 s and 0.02 Hz, respectively. The Gaussian function fit provided the central frequencies, ω_m, and the spectral semibandwidths, $\delta\omega$. The total wave magnetic power, δB^2, was estimated for each wave packet by summing the power spectral density bins in the range $\omega_m \pm \delta\omega$ and then multiplying the result by $\delta\omega$. Using the full wave spectral range, *Loto'aniu et al.* [2006] found that electrons with $E \leq 2$ MeV could interact with only three wave packets (16, 17, and 19) if storm-time ion concentration was assumed (70% H^+, 20% He^+, and 10% O^+). Those packets were the He^+-mode EMIC waves, and for the calculation below, we selected two of them. The associated plasma and wave characteristics are summarized in Table 1. Note that to generate this table, we used the definition of full width at half maximum (FWHM) as it was given by Loto'aniu et al., that is, FWHM = $2\sqrt{2\ln 2}\,\delta\omega$, despite the Gaussian fit $\sim\exp\{-(\omega - \omega_m)^2/\delta\omega^2\}$. Of the packets 16, 17, and 19, wave packet 16 has the most narrow distribution and 19 has the widest distribution, with corresponding power spectral densities presented in Figure 3.

[18] To show the effect of the wave-normal angle distribution on relativistic electron scattering, we use the wave-normal angle distributions from equation (2), and in addition, a storm-time ion concentration is assumed. For reference purposes, we also calculate the diffusion coefficients for strictly parallel/antiparallel propagating EMIC waves. For each wave packet, the power spectral density is normalized to the corresponding wave magnetic power δB^2 shown in Table 1, and this normalization is kept the same for any particular wave-normal angle distribution (see equation (2)). In order to estimate the minimum resonant energy, we use y_{UC} from Table 1. For strictly field-aligned wave propagation, as follows from Figure 2, the energy is about 2 MeV for both wave packets (we can use Figure 2 for wave packet 19 because ω_{pe}/Ω_e was nearly the same during both). This minimum resonant energy exceeds the values presented by *Loto'aniu et al.* [2006], especially for wave packet 16; for this packet and a storm-time ion concentration, they obtained E_{min} = 0.2 MeV that, as follows from Figure 2, corresponds to a y_{UC} about 0.2496.

[19] Figure 4 shows the results of our calculation for wave packet 16. For strictly parallel wave propagation, the minimum resonant energy is only slightly below 2 MeV, and the diffusion coefficients for field-aligned and interme-

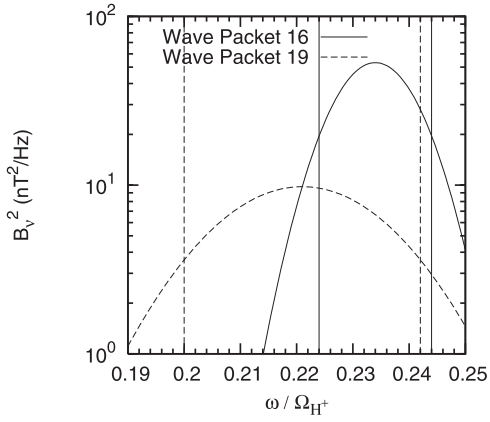

Figure 3. Transverse power spectral densities for wave packets 16 and 19 obtained by *Loto'aniu et al.* [2006]. The solid and dashed vertical lines restrict the frequency range $\omega_m \pm \delta\omega$ for packets 16 and 19, respectively.

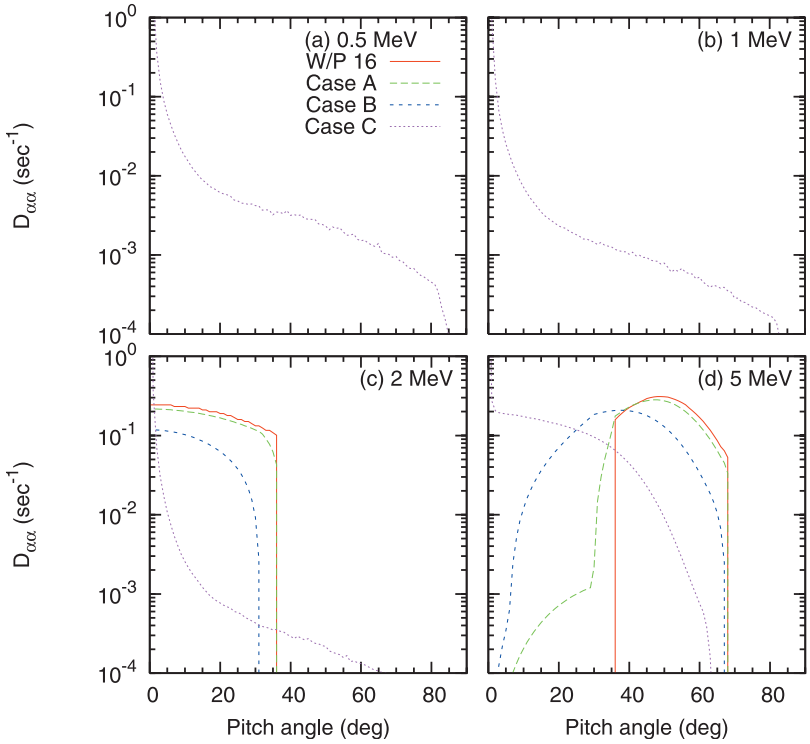

Figure 4. Local pitch angle diffusion coefficients for wave packet 16. Calculations are based on a storm-time ion composition, $\eta_{H^+} = 0.7$, $\eta_{He+} = 0.2$, and $\eta_{O+} = 0.1$. "W/P 16" shows the results for strictly parallel-antiparallel propagating He^+-modes, and Cases A, B, and C are obtained for the corresponding wave-normal angle distribution given by equation (2).

diate wave propagation are only nonzero in Figures 4c and 4d. Cases A and B demonstrate results similar to Figures 1b and 1c. Because y_{UC} is very close to the He^+ gyrofrequency, the minimum resonant energy falls below 1 MeV if the wave-normal angle exceeds 88°, so that Case C may potentially scatter such low-energy electrons with an appreciable rate as shown in Figures 4a and 4b. Another feature of highly oblique waves is clearly observed in Figures 4d where the range of pitch angle diffusion is substantially extended down to the loss cone. While Case C exhibits a quite different behavior compared to Figure 1, there is a similarity between the diffusion coefficients in Figures 1c and 4d.

[20] The diffusion coefficients for wave packet 19 are shown in Figure 5. Both Figures 5c and 5d are quite similar and demonstrate qualitatively the same behavior as in Figures 1a and 1b. As follows from Figures 5a and 5b, Case C practically does not scatter low-energy electrons, mainly because of a lower y_{UC} for wave packet 19 than in Figure 4.

3.3. Cyclotron Damping Near He^+ Gyrofrequency and its Consequence for Electron Scattering

[21] As follows from Table 1, y_{UC} is very close to the local He^+ gyrofrequency ($y_{He+} = 0.25$) for both wave packets. In this frequency region, the He^+-mode experiences strong cyclotron damping due to interaction with thermal He^+ [e.g., *Akhiezer et al.*, 1975]. To demonstrate this, we assume the He^+ temperature to be $T_{He^+} = 1$ eV, and present in Figure 6 the wave damping rate for the storm-time ion composition and plasma parameters observed during wave packet 16. The frequency range shown covers approximately the entire wave packet 16. The damping rate for y_{LC} has only a narrow peak for $\theta > 89°$, and this region is excluded from the calculation of the diffusion coefficients (see equation (2)). For y_m, the region of damping near 90° extends slightly below 89°, and in addition, small damping appears for a field-aligned wave propagation. The situation becomes dramatically different for y_{UC} when the He^+-mode experiences strong damping in the entire wave-normal angle region; the energy damping time is $0.5/\gamma_{He+} \approx 7$ s, which is only four times greater than the wave period. In all cases, substantial damping takes place only if $|y - 0.25| \lesssim k_{\|} v_{\|,He+}/\Omega_{H+}$, where $v_{\|,He+}$ is the field-aligned temperature of He^+. Moreover, we employ a "cold plasma" approximation in our diffusion coefficient software (as was done by *Loto'aniu et al.* [2006]), some must check the validity of this approximation. Particularly, the inequality

$$|y - 0.25| >> \frac{k_{\|} v_{\|,He^+}}{\Omega_{H^+}} = \varepsilon_{th} \qquad (6)$$

should hold.

[22] Inequality (6) is extremely crucial for the diffusion coefficient calculation because thermal effects should be considered if inequality (6) is violated, but more importantly, the He^+-mode damps strongly in the region $|y - 0.25| \lesssim \varepsilon_{th}$. For wave packets 16 and 19, inequality (6) is strongly violated in the vicinity of y_{UC}, and waves cannot exist in these frequency regions, which for $T_{He+} = 1$ eV are the ranges $\varepsilon_{th} = 5 \times 10^{-3} - 9 \times 10^{-2}$ and $\varepsilon_{th} = 3 \times 10^{-3} - 6 \times 10^{-2}$,

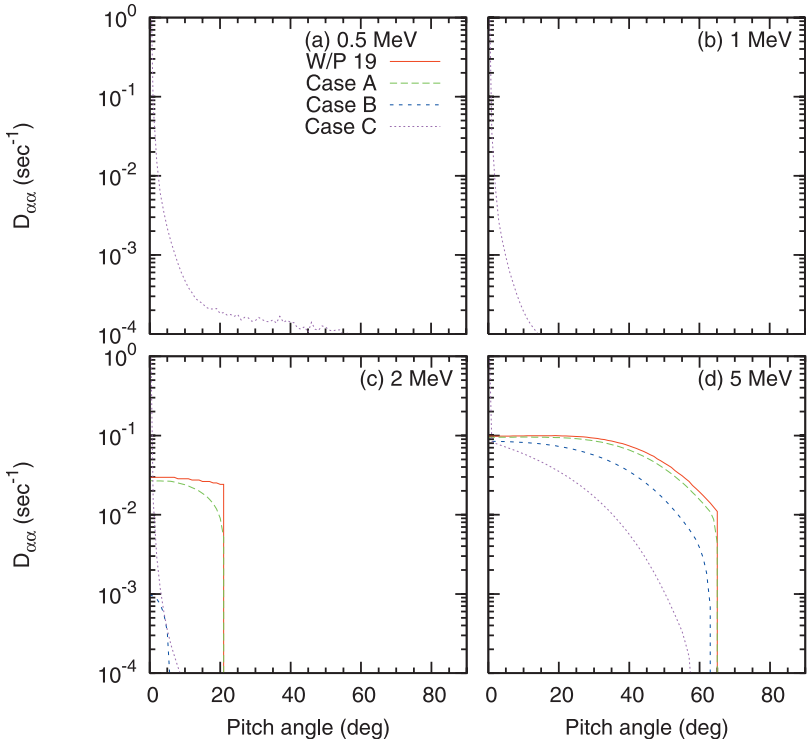

Figure 5. Same as Figure 4, except for wave packet 19.

respectively. Using these numbers and Table 1, we conclude that, in order to suppress cyclotron damping completely, the He^+ temperature should be decreased at least by 1/80 for wave packet 16, and at least by 1/40 for wave packet 19. Any reasonable change to the temperature assumed in our calculation cannot eliminate the effect and can only influence the frequency range subject to cyclotron damping.

[23] Our conclusion that EMIC waves experience strong cyclotron damping near the He^+ gyrofrequency contradicts the results of *Loto'aniu et al.* [2006] because these authors estimated all their y_{UC} values from CRRES data (after filtering, FFT, and Gaussian approximations). Unfortunately, we do not know all the details regarding the data processing used by Loto'aniu et al., but we know that the wave frequency resolution in their data was 0.02 Hz. This uncertainty provides the ranges $(y_{LC},y_{UC}) = (0.20–0.25,0.22–0.27)$ and $(y_{LC},y_{UC}) = (0.17–0.22,0.22–0.27)$ for wave packets 16 and 19, respectively, that can reconcile our theoretical result with the data reported by Loto'aniu et al.. So we do not see any reason inequality (6) is violated, and it must be taken into account.

[24] Let us now recalculate the diffusion coefficients presented in Figure 4, neglecting contributions from all the partial diffusion coefficients if $|y - 0.25| \leq \varepsilon_{th}$ (keeping all parameters the same). Note that all the results presented in Figure 1 are still valid because inequality (6) holds for all those parameters. The results of the recalculation are presented in Figure 7, and there is a qualitative difference in comparison to Figure 4. Now, for all wave-normal angle distributions, low-energy electron pitch angle diffusion is not possible, and while the 2 MeV diffusion coefficients are nonzero in Figure 7c, they are at least partly inside the equatorial loss cone for $L \approx 7.3$. For greater electron energies, the contribution from the high frequency part of the wave power spectral density decreases. As a result, Figures 4d and 7d look similar except that diffusion vanishes at slightly lower pitch angles in Figure 7d than in Figure 4d, and the transition between $|n| = 1$ and $|n| = 2$ resonances is not continued in Figure 7d for Case A.

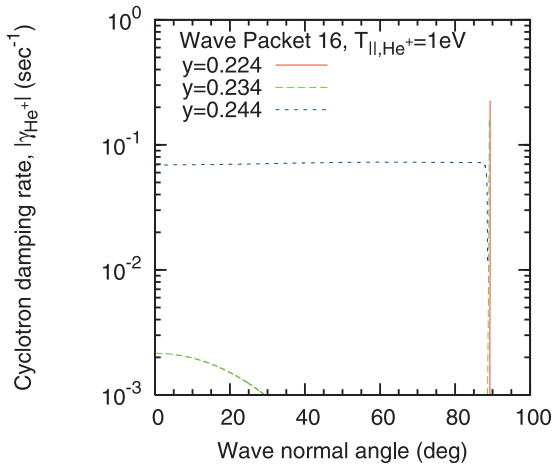

Figure 6. The He^+-mode damping rate due to interaction with thermal He^+. The phase space distribution function for He^+ is Maxwellian with $T_{He+} = 1$ eV, but thermal effects are neglected in the real part of the dispersion relation. All other plasma species are described in a "cold plasma" approximation. A storm-time ion composition is assumed, and the plasma density and magnetic field are taken from the work of *Loto'aniu et al.* [2006, wave packet # 16].

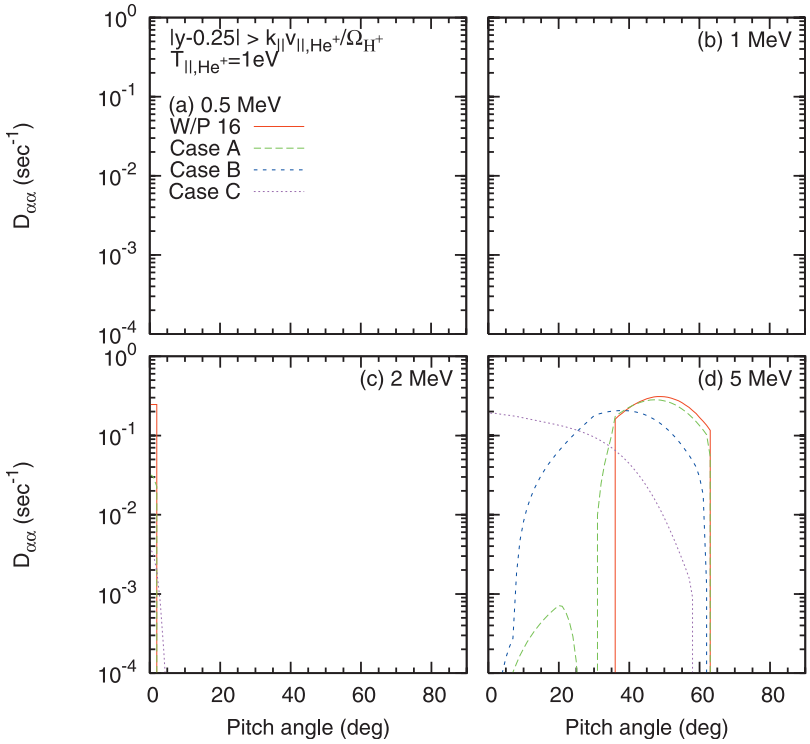

Figure 7. Same as Figure 4, except inequality $|y - 0.25| > k_{\|} v_{\|,\mathrm{He}^+}/\Omega_{\mathrm{H}^+}$ is held during the diffusion coefficient calculations.

[25] The results of our recalculation for wave packet 19 are shown in Figure 8. Similar to wave packet 16, diffusion is not possible for low energies, and Figures 5d and 8d are very similar.

[26] In conclusion, we emphasize that, as we demonstrated above, the He^+-mode does not experience significant cyclotron damping by thermal He^+ if $y \lesssim y_{\mathrm{m}}$ (see Figure 6). So the observed changes in the diffusion coefficients are

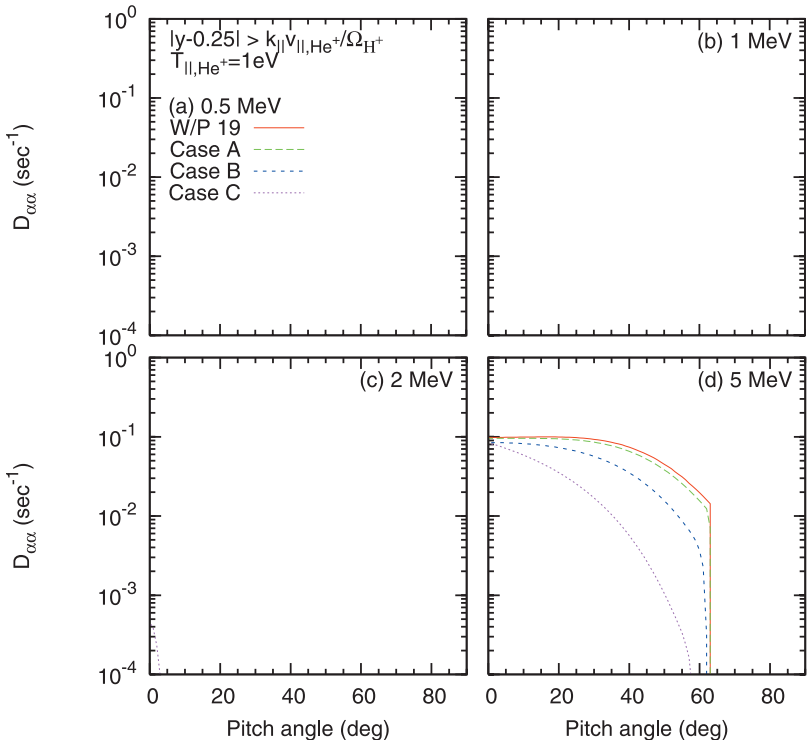

Figure 8. Same as Figure 5, except inequality $|y - 0.25| > k_{\|} v_{\|,\mathrm{He}^+}/\Omega_{\mathrm{H}^+}$ is held during the diffusion coefficient calculations.

due to the frequency region near y_{UC}, and qualitatively correct diffusion coefficients may be obtained by only considering the region $y \lesssim y_m$. This result is consistent with the conclusions of *Meredith et al.* [2003] regarding the electron minimum resonant energy which were obtained by considering only the central wave packet frequencies, and suggests that the number of EMIC wave packets that are able to interact with electrons below 2 MeV may significantly decrease compared with the estimate of *Loto'aniu et al.* [2006].

4. Summary and Conclusions

[27] Precipitation of outer RB electrons due to resonant pitch angle scattering by EMIC waves is considered to be one of the most important loss mechanisms. The effectiveness of relativistic electron scattering depends strongly on the EMIC wave spectral properties, but unrealistic assumptions regarding the wave angular spread were made in previous theoretical studies. Namely, only strictly field-aligned or quasi-field-aligned waves were considered [*Summers and Thorne*, 2003; *Albert*, 2003; *Loto'aniu et al.*, 2006]. The effect of oblique EMIC waves on relativistic electron scattering was recently discussed by *Glauert and Horne* [2005]. For prescribed plasma and wave parameters, considering the H^+-mode EMIC waves, they calculated the local diffusion coefficients and demonstrated that when a realistic angular spread of propagating waves is taken into account, electron diffusion at ~0.5 MeV is only slightly reduced compared to the assumption of field-aligned propagation, but at ~5 MeV, electron diffusion at pitch angles near 90° is reduced by a factor of 5 and increased by several orders of magnitude at pitch angles 30°–80°. Thus at energies of a few megaelectronvolts, the assumption of field-aligned wave propagation breaks down, significantly overestimates the pitch angle diffusion coefficient at large pitch angles, and underestimates the local diffusion rate at smaller pitch angles by orders of magnitude.

[28] The purpose of the present study was to consider the impact of oblique EMIC waves on local relativistic electron scattering using simultaneous observations of plasma and wave parameters from CRRES, and to estimate the effect of bounce averaging. Analyzing 25 EMIC wave packets and considering the full wave spectral range, *Loto'aniu et al.* [2006] found that electrons with $E \leq 2$ MeV could interact with wave packets 16, 17, and 19 only if a storm-time ion concentration is assumed (70% H^+, 20% He^+, and 10% O^+). Those packets were He^+-mode EMIC waves, where we have selected wave packets 16 and 19 for our analyses. Results of our study can be summarized as follows:

[29] 1. In comparison with the field-aligned waves, the intermediate and highly oblique distributions slightly decrease the pitch angle range subject to diffusion, and reduce the local scattering rate by about an order of magnitude at pitch angles where the principle $|n| = 1$ resonances operate (see Figures 7 and 8). Oblique waves allow the $|n| > 1$ resonances to operate, extending the range of local pitch angle diffusion down to the loss cone, and increasing the diffusion at lower pitch angles by orders of magnitude (see Figures 7d).

[30] 2. The local diffusion coefficients based on concurrent plasma/wave parameters from CRRES are qualitatively similar to the results obtained for defined plasma parameters with model wave spectra (compare Figures 7 and 8 with the first row in Figure 1). So we anticipate that the bounce-averaged diffusion coefficients, if estimated from concurrent wave/particle data, will exhibit dependencies similar to those we found for the model bounce-averaged calculations (see Figure 1, the third row). Those dependencies are as follows. First, for low-energy electrons, if only principal $|n| = 1$ resonances operate, intermediate and highly oblique wave distributions (in contrast to field–aligned waves) reduce the equatorial pitch angle range subject to diffusion and decrease the bounce-averaged scattering rate near the edge of the equatorial loss cone by orders of magnitude. This low-energy threshold depends on specified plasma and/or wave parameters, which is $E \approx 2$ MeV for parameters used in Figure 1. Second, for greater electron energies, the $|n| = 1$ resonances operate only in a narrow region at large pitch angles (see Figures 1c and 1d), but due to significant scattering at higher latitudes, the bounce-averaged diffusion coefficients for field-aligned waves extend down to the equatorial loss cone. For these energies, oblique waves operating at $|n| > 1$ resonances are more effective and provide nearly the same bounce-averaged scattering rate in the vicinity of the loss cone as field-aligned waves do (see Figures 1c and 1d, the third row).

[31] **Acknowledgments.** This research was performed while K. Gamayunov held a NASA Postdoctoral Program appointment at NASA/MSFC. Funding in support of this study was provided by NASA grant UPN 370-16-10, NASA HQ POLAR Project, and NASA LWS Program.

[32] Wolfgang Baumjohann thanks the reviewers for their assistance in evaluating this paper.

References

Akhiezer, A. I., I. A. Akhiezer, R. V. Polovin, A. G. Sitenko, and K. N. Stepanov (1975), *Plasma Electrodynamics*, vol. 1, Elsevier, New York.

Albert, J. M. (2003), Evaluation of quasi-linear diffusion coefficients for EMIC waves in a multispecies plasma, *J. Geophys. Res.*, *108*(A6), 1249, doi:10.1029/2002JA009792.

Foat, J. E., et al. (1998), First detection of a terrestrial MeV X-ray burst, *Geophys. Res. Lett.*, *25*, 4109–4112.

Glauert, S. A., and R. B. Horne (2005), Calculation of pitch angle and energy diffusion coefficients with the PADIE code, *J. Geophys. Res.*, *110*, A04206, doi:10.1029/2004JA010851.

Green, J. C., T. G. Onsager, T. P. O'Brien, and D. N. Baker (2004), Testing loss mechanisms capable of rapidly depleting relativistic electron flux in the Earth's outer radiation belt, *J. Geophys. Res.*, *109*, A12211, doi:10.1029/2004JA010579.

Khazanov, G. V., K. V. Gamayunov, and V. K. Jordanova (2003), Self-consistent model of magnetospheric ring current ions and electromagnetic ion cyclotron waves: The 2–7 May 1998 storm, *J. Geophys. Res.*, *108*(A12), 1419, doi:10.1029/2003JA009856.

Khazanov, G. V., K. V. Gamayunov, D. L. Gallagher, and J. U. Kozyra (2006), Self-consistent model of magnetospheric ring current and propagating electromagnetic ion cyclotron waves: Waves in multi ion magnetosphere, *J. Geophys. Res.*, *111*, A10202, doi:10.1029/2006JA011833.

Khazanov, G. V., K. V. Gamayunov, D. L. Gallagher, J. U. Kozyra, and M. W. Liemohn (2007), Self-consistent model of magnetospheric ring current and propagating electromagnetic ion cyclotron waves: 2. Wave induced ring current precipitation and thermal electron heating, *J. Geophys. Res.*, *112*, A04209, doi:10.1029/2006JA012033.

Kim, H.-J., and A. A. Chan (1997), Fully adiabatic changes in storm time relativistic electron fluxes, *J. Geophys. Res.*, *102*, 22,107–22,116.

Li, X., et al. (1997), Multi-satellite observations of the outer zone electron variation during the November 3–4, 1993, magnetic storm, *J. Geophys. Res.*, *102*, 14,123–14,140.

Lorentzen, K. R., M. P. McCarthy, G. K. Parks, J. E. Foat, R. M. Millan, D. M. Smith, R. P. Lin, and J. P. Treilhou (2000), Precipitation of rela-

tivistic electrons by interaction with electromagnetic ion cyclotron waves, *J. Geophys. Res.*, *105*, 5381–5389.

Loto'aniu, T. M., R. M. Thorne, B. J. Fraser, and D. Summers (2006), Estimating relativistic electron pitch angle scattering rate using properties of the electromagnetic ion cyclotron wave spectrum, *J. Geophys. Res.*, *111*, A04220, doi:10.1029/2005JA011452.

Lyons, L. R., and R. M. Thorne (1972), Parasitic pitch angle diffusion of radiation belt particles by ion cyclotron waves, *J. Geophys. Res.*, *77*, 5608–5616.

Meredith, N. P., R. B. Horne, D. Summers, R. M. Thorne, R. H. A. Iles, D. Heynderickx, and R. R. Anderson (2002), Evidence for acceleration of outer zone electrons to relativistic energies by whistler mode chorus, *Ann. Geophys.*, *20*, 967–979.

Meredith, N. P., R. M. Thorne, R. B. Horne, D. Summers, B. J. Fraser, and R. R. Anderson (2003), Statistical analysis of relativistic electron energies for cyclotron resonance with EMIC waves observed on CRRES, *J. Geophys. Res.*, *108*(A6), 1250, doi:10.1029/2002JA009700.

Millan, R. M., R. P. Lin, D. M. Smith, K. R. Lorentzen, and M. P. McCarthy (2002), X-ray observations of MeV electron precipitation with a balloon-borne germanium spectrometer, *Geophys. Res. Lett.*, *29*(24), 2194, doi:10.1029/2002GL015922.

Reeves, G. D., K. L. McAdams, R. H. W. Friedel, and T. P. O'Brien (2003), Acceleration and loss of relativistic electrons during geomagnetic storms, *Geophys. Res. Lett.*, *30*(10), 1529, doi:10.1029/2002GL016513.

Shprits, Y. Y., W. Li, and R. M. Thorne (2006), Controlling effect of the pitch angle scattering rates near edge of the loss cone on electron lifetimes, *J. Geophys. Res.*, *111*, A12206, doi:10.1029/2006JA011758.

Summers, D., and R. M. Thorne (2003), Relativistic electron pitch-angle scattering by electromagnetic ion cyclotron waves during geomagnetic storms, *J. Geophys. Res.*, *108*(A4), 1143, doi:10.1029/2002JA009489.

Summers, D., C. Ma, and T. Mukai (2004), Competition between acceleration and loss mechanisms of relativistic electrons during geomagnetic storms, *J. Geophys. Res.*, *109*, A04221, doi:10.1029/2004JA010437.

Summers, D., B. Ni, and N. P. Meredith (2007), Timescales for radiation belt electron acceleration and loss due to resonant wave-particle interactions: 2. Evaluation for VLF chorus, ELF hiss, and electromagnetic ion cyclotron waves, *J. Geophys. Res.*, *112*, A04207, doi:10.1029/2006JA011993.

Thorne, R. M., and R. B. Horne (1992), The contribution of ion-cyclotron waves to electron heating and SAR-arcs excitation near the storm-time plasmapause, *Geophys. Res. Lett.*, *19*, 417–420.

Thorne, R. M., and C. F. Kennel (1971), Relativistic electron precipitation during magnetic storm main phase, *J. Geophys. Res.*, *76*, 4446–4453.

Thorne, R. M., R.B. Horne, S. A. Glauert, N. P. Meredith, Y. Y. Shprits, D. Summers, and R. R. Anderson (2005), The influence of wave-particle interactions on relativistic electron dynamics during storms, in *Inner Magnetosphere Interactions: New Perspectives From Imaging, Geophys. Monogr. Ser.*, vol. 159, edited by J. Burch, M. Schulz, and M. Spence, pp. 101–112, AGU, Washington, D.C.

K. V. Gamayunov and G. V. Khazanov, National Space Science and Technology Center VP62, NASA Marshall Space Flight Center, Space Science Department, 320 Sparkman Drive, Huntsville, AL 35805, USA. (konstantin.gamayunov@msfc.nasa.gov; george.khazanov@msfc.nasa.gov)